Environmental Research 159 (2017) 124–134

Contents lists available at ScienceDirect

Environmental Research

journal homepage: www.elsevier.com/locate/envres

Grassland productivity and carbon sequestration in Mongolian grasslands: The underlying mechanisms and nomadic implications

Changliang Shao[a], Jiquan Chen[b,*], Housen Chu[c], Raffaele Lafortezza[b,d], Gang Dong[e], Michael Abraha[b], Ochirbat Batkhishig[f], Ranjeet John[b], Zutao Ouyang[b], Yaoqi Zhang[g], Jiaguo Qi[b]

[a] Institute of Agricultural Resources and Regional Planning, Chinese Academy of Agricultural Sciences, Beijing 100081, China
[b] Center for Global Change & Earth Observations (CGCEO), Michigan State University, East Lansing, MI 48823, USA
[c] Department of Environmental Science, Policy, and Management, University of California, Berkeley, CA 94720, USA
[d] Department of Agricultural and Environmental Sciences, University of Bari, Bari 70126, Italy
[e] School of Life Science, Shanxi University, Taiyuan 030006, China
[f] Institute of Geography, Mongolian Academy of Sciences, Ulaanbarrtar 210620, Mongolia
[g] School of Forestry and Wildlife Sciences, Auburn University, Auburn, AL 36949, USA

ARTICLE INFO

Keywords:
Global warming
Global change
Carbon emission
Ecosystem function
Eddy-covariance

ABSTRACT

Background: Quantifying carbon (*C*) dioxide exchanges between ecosystems and the atmosphere and the underlying mechanism of biophysical regulations under similar environmental conditions is critical for an accurate understanding of *C* budgets and ecosystem functions.

Methods: For the first time, a cluster of four eddy covariance towers were set up to answer how *C* fluxes shift among four dominant ecosystems in Mongolia – meadow steppe (MDW), typical steppe (TPL), dry typical steppe (DRT) and shrubland (SHB) during two growing seasons (2014 and 2015).

Results: Large variations were observed for the annual net ecosystem exchange (NEE) from 59 to 193 g C m^{-2}, though all four sites acted as a *C* source. During the two growing seasons, MDW acted as a *C* sink, TPL and DRT were *C* neutral, while SHB acted as a *C* source. MDW to SHB and TPL conversions resulted in a 2.6- and 2.2-fold increase in *C* release, respectively, whereas the TPL to SHB conversion resulted in a 1.1-fold increase at the annual scale. *C* assimilation was higher at MDW than those at the other three ecosystems due to its greater *C* assimilation ability and longer *C* assimilation times during the day and growing period. On the other hand, *C* release was highest at SHB due to significantly lower photosynthetic production and relatively higher ecosystem respiration (ER). A stepwise multiple regression analysis showed that the seasonal variations in NEE, ER and gross ecosystem production (GEP) were controlled by air temperature at MDW, while they were controlled mainly by soil moisture at TPL, DRT and SHB. When air temperature increased, the NEE at MDW and TPL changed more dramatically than at DRT and SHB, suggesting not only a stronger *C* release ability but also a higher temperature sensitivity at MDW and TPL.

Conclusions: The ongoing and predicted global changes in Mongolia likely impact the *C* exchange at MDW and TPL more than at DRT and SHB in Mongolia. Our results suggest that, with increasing drought and vegetation type succession, a clear trend for greater CO_2 emissions may result in further global warming in the future. This study implies that diverse grassland ecosystems will respond differently to climate change in the future and can be seen as nature-based solutions (NBS) supporting climate change adaptation and mitigation strategies.

1. Introduction

Promoted by the European Union (EU), the concept of nature-based solutions (NBS) is becoming the dominant school of thought in planning and managing socioecological systems (SES) toward sustainability (European Commission, 2010; Maes and Jacobs, 2015). It advances conventional ecosystem management by focusing on society and human wellbeing. Eggermont et al. (2015) stated that NBS "refer to the sustainable management and use of nature for tackling societal challenges". While the primary target of the EU's mission was human-dominated systems (e.g., urban areas, European Commission, 2010), the NBS concept seems readily applicable for rural ecosystems. One of the best examples are the dryland regions, where herders are highly dependent on nature for their nomadic practices to sustain the livestock

* Corresponding author.
E-mail address: jqchen@msu.edu (J. Chen).

http://dx.doi.org/10.1016/j.envres.2017.08.001
Received 16 November 2016; Received in revised form 29 July 2017; Accepted 1 August 2017
Available online 08 August 2017

(Dangal et al., 2016; John et al., 2016), which in turn determines the stability of the herders' societal and individual wellbeing. Herders migrate with their livestock across the landscape based on grassland quantity (e.g., cover type and area) and quality (e.g., productivity). From a scientific perspective, a mechanistic understanding and accurate prediction of productivity in dominant grasslands would be a first step in assisting with the herders' management activities (Dangal et al., 2016). Unfortunately, our current capability in predicting the spatiotemporal changes of grasslands on drylands lag significantly behind other biomes (e.g., forests), and are mostly based on model predictions and/or remote sensing products (Yuan et al., 2007; Hilker et al., 2014; Zhang et al., 2014; Dangal et al., 2016). For example, in situ direct measurements of gross ecosystem productivity (GEP) using flux towers in drylands remain scarce across the globe (Kato and Tang, 2008; Li et al., 2013; Xiao et al., 2013; Ahlström et al., 2015), regardless of their high sensitivity to the changing climate and human disturbances (Chen et al., 2013).

Vast grasslands account for ~ 60% of the Mongolian Plateau, with a total area of ~1.56 million km^2; however, approximately 3 million people live there. Because Mongolia is land locked, there exists a much tighter relationship between its people and nature. This is especially true for the nomadic herders who have traditionally roamed based on grassland productivity, water, etc. (Fernández-Giménez et al., 2012; Chen et al., 2015b). Intense human activities and rapid change in climate over recent decades have produced serious ecological (IPCC, 2014; Liu et al., 2014; Shao et al., 2014; Shao et al., 2017) and socioeconomic (Groisman and Soja, 2009; Qi et al., 2012, 2017; Chen et al., 2015a) consequences at both local and regional scales, such as the higher-than-average global warming rate on the plateau (John et al., 2009; Lu et al., 2009), a decreased trend in summer precipitation and an increased trend in spatial variability (John et al., 2016), and increased livestock density (Chen et al., 2015b). Worse yet, the IPCC (2014) has predicted that this water-limited region will experience a warming trend that is higher than the global mean, which would further alter summer and winter precipitation patterns and increase the frequency of extreme climatic events (Qu et al., 2016). Scientists and policy makers are becoming increasingly interested in the spatiotemporal changes of grassland productivity and/or *C* sequestration strength (Xie et al., 2014; Abraha et al., 2016; Lafortezza and Chen, 2016; Luo and Wu, 2016). However, direct measurements of *C* sequestration in Mongolia have received little attention, with most literature based on model predictions (including remote sensing modeling). To our knowledge, literature reports only a one-year eddy covariance (EC) measurement (i.e., Li et al., 2005) for this vast landscape.

Spatiotemporal changes of the dominant vegetation types on the Mongolian Plateau (e.g., meadow, dry steppe, and shrubland) have occurred at quite an alarming rate and scale and are expected to significantly increase in upcoming decades (Lioubimtseva and Henebry, 2009; Chen et al., 2015b; Kelley et al., 2015), magnifying the challenges in predicting the spatiotemporal distribution of grassland productivity. For example, total grassland area increased from 33% in 2001 to 42% in 2009 (Chen et al., 2013). John et al. (2009) reported that the sparsely vegetated area increased by 151% from 1992 to 2004, resulting in significant changes in species distribution and vegetation productivity. Our recent analyses based on MCD12Q1 between 2001 and 2012 further confirmed a 77% increase in shrublands for the East Asian dryland (Chen et al., 2013). These changes in vegetation types and distributions would result in direct feedbacks to the regional climate, livestock management, and nomadic cavities on the plateau.

To address the above pressing issues in Mongolia and fill the data gaps, a field experiment was designed for the first time in which a cluster of four EC systems was deployed to directly quantify ecosystem productivity of the dominant ecosystems, including a meadow steppe (MDW), a typical steppe (TPL), a dry typical steppe (DRT), and a shrubland (SHB) (Table 1), so that future upscaling to the region will have a solid foundation. While our long term goal is to develop the capacity to predict grassland productivity for herders upon which they can schedule their nomadic activities, the specific objectives of this study were to: (1) explore the daily, monthly, and seasonal variations in *C* fluxes: GEP, ER and NEE (net ecosystem CO_2 exchange) of the four ecosystems; (2) quantify the biophysical regulations of GEP, ER and NEE within and among the four ecosystems; and (3) diagnose the effect of vegetation change on the GEP, ER and NEE. We hypothesized that GEP would be higher at MDW than at other grassland types because of greater NEE (i.e., more *C* assimilation or less *C* release) than ER. We also predicted that the MDW and TPL are more resistant, or less sensitive, to the changing climate than the DRT and SHB. Lessons learned from this study may provide the first palpable data for nomadic societies to use when developing future management strategies and tactics.

2. Materials and methods

2.1. Study area

The four sites are located in the Ulaanbaatar and TOV provinces of Mongolia (Fig. 1). The region lies in a temperate zone and has a distinct continental climate with an average annual air temperature and precipitation of 1.2 °C and 196 mm, respectively. The growing season from June through September is warm and relatively wet registering an annual precipitation of about 88%, while the remaining months (October-May) are cold and dry. Mean daily temperatures for January and July are −22.9 and 21.4 °C, respectively. Precipitation is quite irregular from one year to the next and shows strong seasonal variability. Frequent droughts are usually the limiting factor for plant growth in this region, which is also characterized by windy conditions. The longest distance among our four study sites is ~200 km between TPL and SHB.

MDW is a permafrost site dominated by *Leymus chinensis* meadow steppe. TPL is comprised of short-grass steppe with cool-season perennial C_3 grasses—*Stipa krylovii* and *Artemisia frigida* – as the dominant species. DRT is dominated by a perennial grass—*Achnatherum splendens*, a widely distributed cover type with overgrazing, while SHB is dominated by *Caragana stenophylla* shrub (Table 1). All four sites are flat with relatively homogenous vegetation, of which the dominant species contributes >80% of the cover. The soil is classified as chestnut soil (FAO) with a sand loamy texture.

2.2. Flux and micrometeorological measurements

Four open-path EC systems, each consisting of an infrared gas analyzer (IRGA, LI-7500, LI-COR, Lincoln, NE) and a CSAT3 three-dimensional sonic anemometer (Campbell Scientific Inc. (CSI), Logan, UT), were deployed 2.0 m above ground to obtain NEE, latent heat (LE) and sensible heat (*H*) fluxes. The raw time series (TS) of three-dimensional wind velocities, sonic temperature, and CO_2 and H_2O concentrations were sampled at a 10 Hz frequency. The IRGA was calibrated before field setup and at the beginning of the growing season each year.

Micrometeorological measurements included photosynthetically active radiation (PAR) (LI-190, LI-COR), net radiation (R_n) (CNR4, Kipp & Zonen, Delft, Netherlands), relative humidity (RH) and air temperature (T_a) (HMP45C, CSI) 2.0 m above ground. Rainfall was measured with tipping bucket rain gauges (TE-525, CSI). Soil temperature (T_s) was measured at 0.05 and 0.10 m depths with eight CS107 probes (CSI). The top 0.30 m averaged volumetric soil water content (SWC) was measured using eight vertically inserted CS616 probes (CSI). Soil heat flux (*G*) was measured at twelve locations using heat flux plates (HFT3.1, CSI) placed 0.02 m below the ground surface. Instrument maintenance was performed biweekly, and the online-computed mean half-hourly scalar fluxes and micrometeorological

Table 1
Geographic location, community height (cm), coverage (%), leaf area index (LAI), green above ground biomass (GNPP, g m^{-2}), and standing dead and litter biomass (g m^{-2}) of the peak growing period in 2014 at the meadow (MDW), typical steppe (TPL), dry typical steppe (DRT) and shrubland (SHB). Values are shown as mean ± SD (n = 4). Significant differences between ecosystems are indicated by different letters (a,b and c) at P = 0.05.

Site name (ab.)	MDW	TPL	DRT	SHB
Latitude (N)	47.7533	47.6884	47.8556	47.8770
Longitude (E)	107.4065	107.2657	105.1698	105.3185
Dominant species	*Carex pediformes*	*Stipa krylovii*	*Achnatherum splendens*	*Caragana stenophylla*
	Leymus chinensis	*Artemisia frigida*	*Carex duriuscula*	*Carex duriuscula*
	Poa attenuata	*Potentilla anserina L.*	*Artemisia Adamsii*	*Cleistogenes squarrosa*
	Iris Bungei	*Cleistogenes squarrosa*		*Artemisia frigida*
Canopy height (cm)	25.0 ± 3.5[a]	30.0 ± 3.5[b]	61.3 ± 45.1[c]	23.8 ± 4.1[a]
LAI	0.85 ± 0.09[a]	0.96 ± 0.09[a]	0.98 ± 0.29[b]	0.77 ± 0.15[c]
Canopy coverage (%)	76.3 ± 4.1[a]	70.0 ± 3.5[a]	51.3 ± 23.6[b]	56.3 ± 4.1[b]
GNPP (g m^{-2})	144.2 ± 14.8[a]	125.9 ± 11.1[b]	107.6 ± 33.4[c]	100.6 ± 19.9[c]
Standing dead (g m^{-2})	46.4 ± 8.4[a]	4.5 ± 2.6[b]	8.3 ± 4.9[b]	5.2 ± 3.1[b]
Litter (g m^{-2})	47.5 ± 11.5[a]	71.6 ± 8.4[a]	61.9 ± 16.8[a]	14.1 ± 2.4[b]

observations along with the TS data were recorded using a CR5000 datalogger (CSI).

2.3. Vegetation measurements

Aboveground green net primary production (GNPP), including all green tissues (Shao et al., 2012), standing dead and litter biomass, were measured biweekly by clipping during growing seasons over the two years using four randomly selected 0.5 m × 0.5 m quadrats at the four directions at each site. The mean canopy height and cover were estimated at peak biomass (usually late July or early August, Table 1). The biomass samples were oven dried at 65 °C to a constant weight (≈ 48 h) to obtain biomass estimates. Leaf area index (LAI) was measured by LI-3000 (LI-COR) for the GNPP before drying, or the specific leaf area (SLA) was used to estimate if only GNPP was available.

2.4. Flux calculation, QA/QC and gap-filling

Half-hourly NEE, LE and H were calculated using EdiRe (University of Edinburgh, v1.5.0.32, http://www.geos.ed.ac.uk/abs/research/micromet/EdiRe) following the workflow of Chu et al., (2014, 2015). Raw TS data quality was checked and spikes were removed. The diagnostic signals from CSAT3 and LI-7500 were used to flag periods with instrument malfunction. Time lags between measured scalars and vertical velocity were removed, and the planar fit (PF) method was applied to rotate the three velocity components into the mean streamline coordinate system (Wilczak et al., 2001). The raw sonic temperature was corrected with fluctuations of water vapor concentration. A 30-min blocking average without detrending was used (Moncrieff et al., 2004), and Webb-Pearman-Leuning (WPL) correction was applied to correct air density fluctuation (Webb et al., 1980). The stationarity, integral turbulence characteristics, and friction velocity (u^*) of each 30-min flux were calculated to filter out the periods with poor turbulent development. The u^* threshold was set at 0.1 m s^{-1} (Shao et al., 2008). We performed experiential range checks for each of the physical variables. We also adopted a 7-day moving window in the time series of half-hourly fluxes to detect and filter out erroneous fluxes (>6 times the standard deviation of each window). Lastly, the footprint for each half-

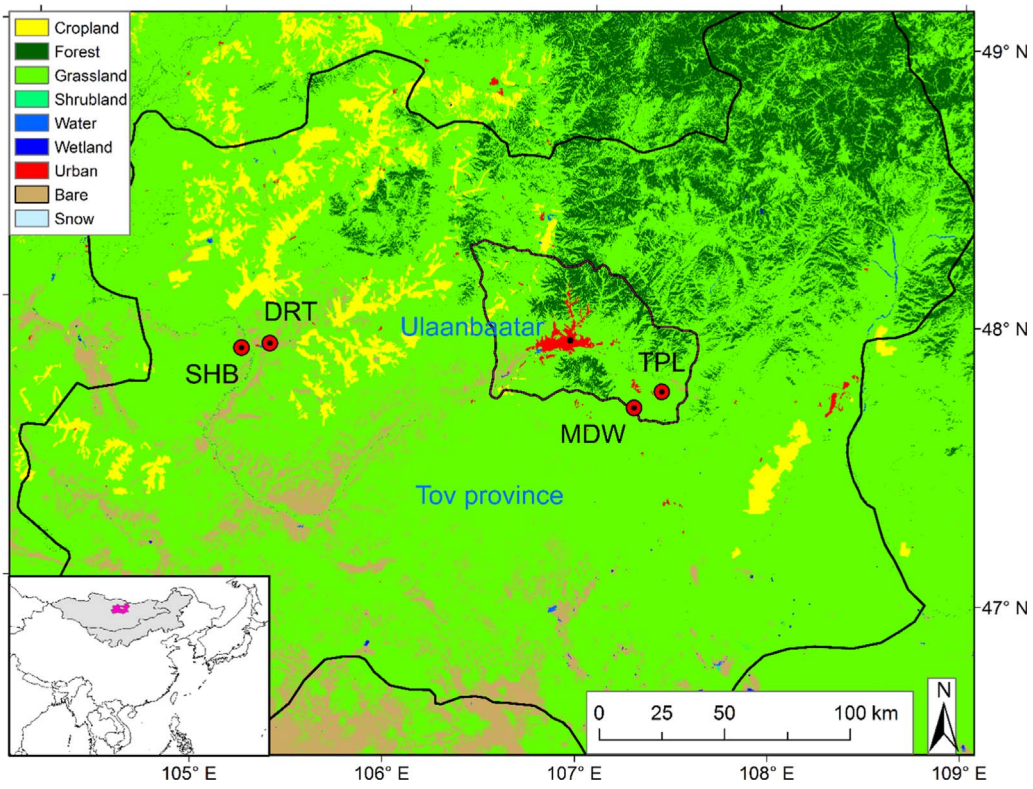

Fig. 1. Locations of the eddy flux measurement sites in the four ecosystems on the Mongolian Plateau – meadow (MDW), typical (TPL), dry typical (DRT) and shrubland (SHB) steppes.

hourly flux was calculated and used to omit periods with < 80% of the measured fluxes originating from measurement fetch (see Section 2.5). To evaluate the performance of the EC systems, energy balance closure (EBC) was conducted with linear regression of the turbulent energy against available energy during the two growing seasons. An EBC of 0.76–0.91 is within normal range for most grassland studies (Wilson et al., 2002; Foken, 2008).

There were 57–63%, 57–63% and 69–81% of NEE, LE and *H*, respectively, classified as "good data", that passed the quality checks as described above. The "good data" were then submitted to directly compare the NEE differences among the four ecosystems or for gap-filling procedures to obtain cumulative fluxes and for flux-partitioning. For the gap-filling, a linear interpolation was first applied for gaps < 1.5 h. The remaining gaps were filled using the marginal distribution sampling (MDS) method by obtaining (1) mean half-hourly values with similar micrometeorological conditions (PAR, VPD, and T_a) within a given window size around the gaps or (2) mean diurnal values from a given window size around the gaps when micrometeorological data were not available. The window size increased from 7 to 14 to 28 days through the iteration of (1) and (2) (Shao et al., 2017). LI-7500 surface heating errors (Burba et al., 2008) were corrected when the sonic temperature reached below − 5 °C because our results showed some differences in NEE and LE only in winter with these corrections (Abraha et al., 2016).

NEE was further partitioned into ER and GEP according to Reichstein et al. (2005). By convention, positive values of NEE indicate a *C* source to the atmosphere, while negative values indicate a *C* sink by the ecosystem. A positive sign was adopted for both GEP and ER (GEP = ER-NEE). The rectangular hyperbola model at 30-min scale was built to describe the partial dependence of the NEE on the PAR, and to obtain the light response curve parameters (Falge et al., 2001):

$$\mathrm{NEE} = \frac{\alpha \times \mathrm{NEE}_{\max} \times \mathrm{PAR}}{\alpha \times \mathrm{PAR} + \alpha \times \mathrm{NEE}_{\max}} + \mathrm{ER}_{\mathrm{day}} \quad (1)$$

where $\mathrm{NEE}_{\max}$ (μmol CO_2 m^{-2} s^{-1}) is the maximum *C* assimilation rate, and $\mathrm{ER}_{\mathrm{day}}$ (μmol CO_2 m^{-2} s^{-1}) is the bulk ER during daytime. α is the ecosystem light use efficiency (μmol CO_2 μmol quanta^{-1}), PAR unit is μmol m^{-2} s^{-1}.

Q_{10} was determined as:

$$Q_{10} = \exp(10b) \quad (2)$$

where *b* is the regression coefficient from nighttime NEE to fit the half-hourly soil temperature at 0.10 m depth (Lloyd and Taylor, 1994):

$$\mathrm{NEE}_{\mathrm{nighttime}} = a \exp(bT_s) \quad (3)$$

2.5. Footprint and uncertainties analysis

The source area of each half-hourly flux was calculated with the footprint model from Kormann and Meixner (2001). We found that 71–78%, 85–90%, and 92–95% of the cumulative fluxes were contributed by areas within 100, 200 and 400 m radii, respectively, centering our towers throughout the study period. Since the towers were far away (>2000 m) from other ecosystems, the influences of other ecosystems on our flux measurements appeared negligible. Thus, our measured fluxes can adequately represent the NEE and energy exchanges of each site. Uncertainties arising from gap filling and u^* threshold, and those computed from Monte Carlo simulations (N = 1000, 95% confidence intervals) were propagated into *C* flux uncertainties (Aurela et al., 2002; Reichstein et al., 2005).

2.6. Data analysis

To isolate the vegetation effects on *C* fluxes by year, we divided the dataset into two years: the first year (Year 1) from June 2014 to May 2015, and the second year (Year 2) from November 2014 to October 2015. Each year included an entire growing season (June-September) and was comparable with other studies. To examine the dependence of key biophysical regulations on *C* exchange among different ecosystems, the NEE–PAR response was first modeled. We grouped the daytime NEE of the growing seasons by T_a ($T_a \leq 10$ °C, 10 °C < $T_a \leq 20$ °C, and $T_a > 20$ °C), VPD (VPD ≤ 1 kPa, 1 kPa < VPD ≤ 2 kPa, and VPD > 2 kPa), and SWC (SWC ≤ 10%, 10% < SWC ≤ 15%, and SWC > 15%) to examine the dependence of the NEE–PAR relationship on these abiotic variables (Fig. 3, Table 3). The NEE data were further grouped by PAR into 100 μmol m^{-2} s^{-1} bins ranging from 0 to 2400 μmol m^{-2} s^{-1} for bin averages. Statistically, this data compilation helped to reduce or offset the errors associated with the measurements resulting from the intermittent natural state of turbulence caused by horizontal transport across large sunny and shaded patches (Falge et al., 2001; Li et al., 2005).

A stepwise multiple regression analysis was performed to investigate the relationships of *C* fluxes with biotic and abiotic variables in SPSS (V22, SPSS Inc., IL, USA). The PF coordinate rotation, gap-filling procedure and other statistical analyses were accomplished with R language (R Development Core Team, 2013 version 3.0.0).

3. Results

3.1. Biotic and abiotic environment

The PAR, T_a, T_s, and VPD showed noticeable differences among the

Table 2
Comparison of growing season and annual level of major meteorological factors and carbon fluxes in the four ecosystems in 2014 and 2015. T_a, mean daily air temperature at 2.0 m height; T_s, mean daily soil temperature at 0.10 m depth; SWC, mean daily soil volumetric water content at 0–0.3 m depth; VPD, mean daily vapor pressure deficit, Rain, rainfall; NEE, net ecosystem CO_2 exchange; ER, ecosystem respiration; GEP, gross ecosystem production; Unc, summed uncertainties.

Item	Growing season (June–September)								Entire year							
	2014				2015				2014				2015			
	MDW	TPL	DRT	SHB	MDW	TPL	DRT	SHB	MDW	TPL	DRT	SHB	MDW	TPL	DRT	SHB
T_a (°C)	12.6	13.3	16.6	16.1	14.2	15.0	18.2	17.8	− 0.6	− 0.3	2.9	1.5	− 0.1	0.2	3.4	2.1
T_s (°C)	10.6	14.4	18.4	20.9	8.5	15.7	19.9	21.1	0.1	0.6	5.8	4.9	− 0.4	1.0	6.2	5.2
SWC (%)	67.3	13.0	6.9	9.5	63.0	8.9	8.4	9.4	38.3	7.7	5.7	7.4	36.9	6.8	6.3	7.4
VPD (kPa)	0.71	0.65	0.89	0.89	0.89	0.88	1.13	1.10	0.45	0.43	0.60	0.56	0.50	0.49	0.64	0.61
Rain (mm)	152	142	127		101	94	79		174	166	144		123	118	96	
NEE (g C m^{-2})	−92	−36	−19	32	−75	32	36	53	**59**	**126**	**139**	**168**	**79**	**187**	**193**	**186**
Unc (g C m^{-2})	23	21	19	20	24	21	20	20	27	26	22	24	29	26	23	24
ER (g C m^{-2})	487	370	259	220	328	181	241	180	**616**	**499**	**410**	**342**	**453**	**309**	**395**	**302**
Unc (g C m^{-2})	23	21	20	20	24	21	20	20	28	26	24	24	29	26	24	25
GEP (g C m^{-2})	579	406	278	188	403	149	205	127	**557**	**373**	**271**	**174**	**374**	**122**	**202**	**116**
Unc (g C m^{-2})	20	19	19	18	21	20	19	19	22	21	21	21	24	22	22	21

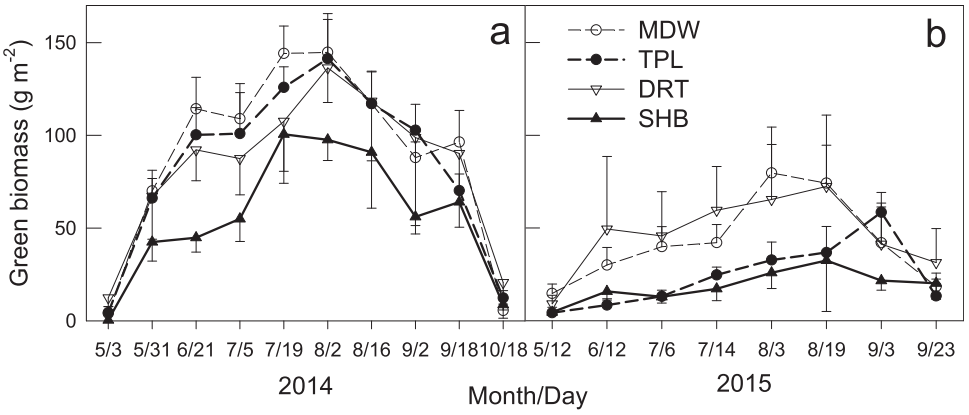

Fig. 2. Seasonal variations of green biomass in the four ecosystems during the two growing seasons in 2014 and 2015.

four sites (Table 2). Growing season T_s at 0.10 m depth was 10.6 °C at MDW, 14.4 °C at TPL, 18.4 °C at DRT, and 20.9 °C at SHB in 2014, which was twice that of MDW, with similar T_s variations in 2015. The T_a showed similar changes to T_s. The SWC was 5–6 times higher at MDW than at all the other three sites that echoed the rainfall events. The VPD at DRT and SHB was greater than that at MDW and TPL in both years. The rainfall events showed clear monthly variability in the first growing season, with 40, 71, 36, and 5 mm from June through September for the four ecosystems, respectively. Most rainfall events were recorded in the early half of the growing season within the critical plant development period in June. In the second growing season, rainfall events of 9, 53 28, and 11 mm were recorded from June through September. Rainfall was one third less in the second growing season than in the first (Table 2).

The GNPP of the four sites showed a unimodal shape in both years, with greater values at MDW than that at SHB (Fig. 2). In late July 2014, the maximum GNPP was 144.2 g m^{-2} for MDW and 125.9 g m^{-2} for TPL, which was significantly ($P < 0.05$) greater than those at DRT (107.6 g m^{-2}) and at SHB (100.6 g m^{-2}). Our vegetation surveys also indicated similar higher canopy cover (70–76%) at MDW and TPL; however, DRT and SHB had significantly ($P < 0.05$) lower cover (51–56%) (Table 1). Additionally, MDW had much more standing dead biomass, while SHB had sparse ground litter compared to the other three ecosystems. The GNPP of DRT was the highest among the four sites in August 2015.

3.2. Diurnal changes of NEE

The diurnal NEE variations for both growing seasons showed the expected daily change with daytime *C* assimilation and night-time *C* release in all four ecosystems (Fig. 3). In June and July of Year 1 and August of Year 2, the NEE moved from *C* release to assimilation after dawn. The *C* assimilation rate was highest around noon, after which it decreased. The NEE switched from a negative to a positive value at dusk. The diurnal *C* assimilation peak time occurred earlier at SHB than at DRT and TPL, while the latest occurrence was at MDW. Conversely, the diurnal *C* assimilation time had a reverse pattern that occurred earlier at MDW than at TPL and DRT while the latest occurrence was at SHB (Fig. 3b and g), demonstrating that MDW had a longer *C* assimilation period during the day than the other three ecosystems. The earliest *C* absorption start period was recorded for MDW as well, while SHB recorded the latest month. The *C* assimilation periods for the two growing seasons were 8, 4, 6, and 3 months at MDW, TPL, DRT and SHB, respectively, showing that MDW had the longest *C* assimilation period during any given year.

The diurnal amplitude of NEE also varied substantially among the four ecosystems (Fig. 3). Generally, the daytime *C* assimilation ability of the canopy was greater at MDW than at TPL and DRT, while it was the lowest at SHB. The most significant daily changes in the four

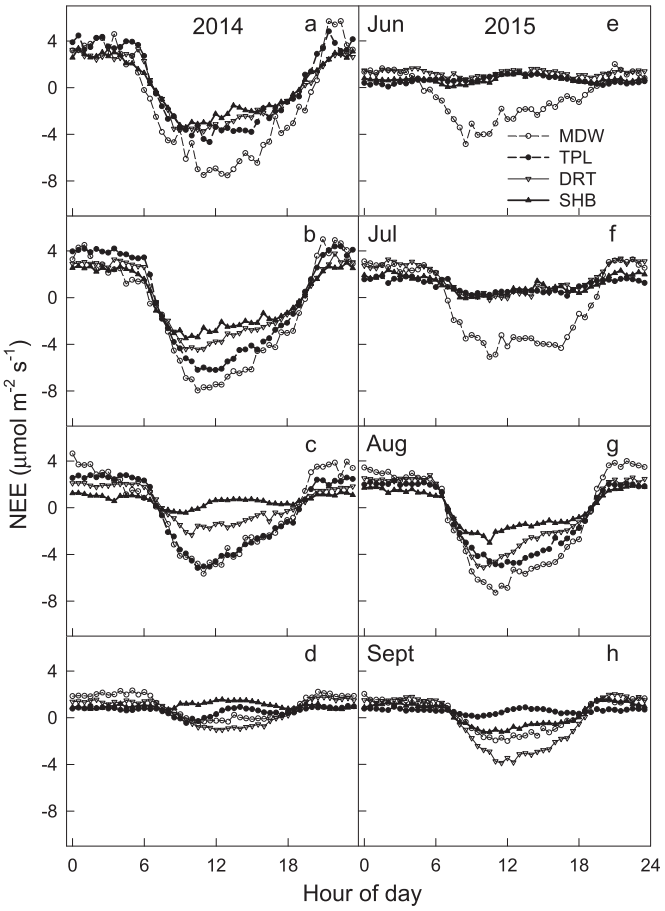

Fig. 3. Monthly average diurnal course of net ecosystem CO_2 exchange (NEE) at the four ecosystems during the two growing seasons in 2014 and 2015.

ecosystems were recorded in July for Year 1 (Fig. 3b) and in August for Year 2 (Fig. 3g). The minimal and maximal NEE of the steppe were −7.9 and 5.4 μmol m^{-2} s^{-1}, respectively, both in July 2014. The peak *C* assimilation at MDW was approximately 2.6-fold the value observed at TPL, 2.8-fold at DRT and 3.5-fold at SHB. Nighttime NEE was low in magnitude relative to daytime NEE, with higher values at MDW and TPL compared to DRT and SHB. Nighttime NEE was higher at MDW than TPL in most months, while it was higher at TPL than MDW during the early and late growing seasons.

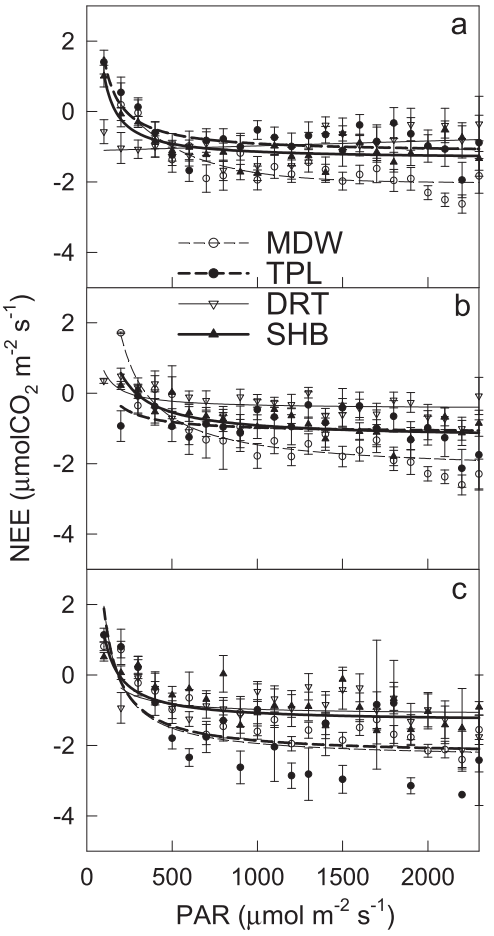

Fig. 4. Daytime net ecosystem CO_2 exchange (NEE) light response curves at the same air temperature (10 °C < T_a ≤ 20 °C, a), soil volumetric water content (SWC > 15%, b), and vapor pressure deficit (1 kPa < VPD < 2 kPa, c) of the four ecosystems during the two growing seasons. Eq. (1) was used to fit the data and the regression coefficients presented in Table 3. The NEE data were grouped by PAR into 100 μmol m^{-2} s^{-1} bins for averages.

3.3. Responses of NEE to abiotic variables

3.3.1. Responses of daytime NEE to PAR

Daytime *C* assimilation increased with PAR at low-to-intermediate levels. However, as PAR exceeded a certain level, the relative decrease in NEE per unit PAR began to change, becoming stable in all four ecosystems, as expected (Fig. 4). There were noticeable differences in the light response curves among different T_a, SWC and VPD conditions and among the four ecosystems (Fig. 4, Table 3). The absolute values of quantum yield (α) were considerably reduced at TPL, DRT and SHB, but increased at MDW with an increase in T_a (Table 3). The model-derived saturated NEE (NEE_{max}) was highest when T_a was optimal. As T_a increased to 20 °C, NEE_{max} was only 28%, 39%, 54% and 66% at MDW, TPL, DRT and SHB, respectively, as opposed to when 10 < T_a ≤ 20 °C. Under the three T_a conditions, NEE_{max} was clearly greater at MDW and SHB than at TPL and DRT. ER_{day} was the highest at MDW when 10 < T_a ≤ 20 °C and at SHB when T_a ≤ 10 °C. The absolute values of both α and NEE_{max} were considerably reduced in a low SWC range. As SWC dropped to < 10%, α was only ~ 50% compared to when SWC was > 10% in TPL, DRT and SHB, while NEE_{max} was only 50%, 38% and 87%, respectively, under 10% SWC conditions. When the water condition was good (> 15%), the NEE_{max} was the highest at TPL; and when the water condition was low (≤ 10%), the NEE_{max} was the highest at SHB. Similarly, both α and NEE_{max} were considerably reduced when the VPD increased. As VPD increased from 1 kPa to 2 kPa, the NEE_{max} dropped to only 30%, 31%, 46% and 40% at MDW, TPL,

Table 3
Estimated coefficients describing the rectangular hyperbolic responses of daytime net ecosystem CO_2 exchange (NEE) to incident PAR (Eq. (1)) at different air temperature (T_a), soil water content (SWC), and vapor pressure deficit (VPD) levels at the four ecosystems during the two growing seasons in 2014 and 2015. NEE_{max}, the saturation value of NEE at an infinite light; ER_{day}, the model-derived bulk ecosystem respiration; α, the apparent quantum yield. NA, data not available.

Variable range	NEE_{max} (μmol CO_2 m^{-2} s^{-1})				ER_{day} (μmol CO_2 m^{-2} s^{-1})				α (μmol CO_2 μmol $quanta^{-1}$)			
	MDW	TPL	DRT	SHB	MDW	TPL	DRT	SHB	MDW	TPL	DRT	SHB
T_a ≤ 10 °C	− 4.4(1.2)	− 2.6(3.5)	− 2.6(2.4)	− 2.8(4.5)	1.1(1.0)	1.9(3.6)	1.6(2.4)	2.1(4.6)	− 0.005(0.005)	− 0.026(0.099)	− 0.027(0.082)	− 0.040(0.017)
10 < T_a ≤ 20 °C	− 7.2(5.1)	− 2.8(1.7)	− 2.6(1.7)	− 3.2(0.6)	4.7(5.3)	1.5(3.3)	1.7(1.7)	1.4(0.7)	− 0.058(0.107)	− 0.002(0.001)	− 0.023(0.048)	− 0.004(0.001)
T_a > 20 °C	− 2.0(9.8)	− 1.1(5.7)	− 1.4(0.7)	− 2.1(0.8)	2.0(9.8)	1.5(2.6)	3.2(2.4)	0.5(0.5)	− 0.129(0.128)	− 0.001(0.021)	− 0.004(0.001)	− 0.001(0.002)
SWC ≤ 10%	NA	− 0.9(2.0)	− 0.8(3.6)	− 2.7(7.1)	NA	0.9(2.0)	1.8(3.0)	2.8(2.6)	NA	− 0.004(0.020)	− 0.006(0.002)	− 0.006(0.003)
10% < SWC ≤ 15%	NA	− 1.8(2.1)	− 2.1(4.8)	− 3.1(3.0)	NA	1.3(2.2)	0.8(2.8)	1.8(1.5)	NA	− 0.010(0.050)	− 0.010(0.004)	− 0.010(0.001)
SWC > 15%	− 4.7(0.6)	− 6.6(3.0)	NA	− 2.7(0.5)	2.1(0.8)	3.6(3.4)	NA	1.0(0.7)	− 0.010(0.008)	− 0.030(0.050)	NA	− 0.005(0.005)
VPD ≤ 1 kPa	− 4.6(0.9)	− 4.2(3.1)	− 3.7(2.6)	− 4.0(1.2)	1.7(1.2)	3.3(3.3)	1.7(3.6)	2.2(1.4)	− 0.009(0.011)	− 0.069(0.026)	− 0.270(0.021)	− 0.027(0.028)
1 kPa < VPD ≤ 2 kPa	− 4.8(2.1)	− 3.0(2.3)	− 2.3(0.5)	− 2.7(0.6)	2.1(2.6)	3.0(3.3)	3.4(2.1)	0.6(0.7)	− 0.010(0.010)	− 0.044(0.024)	− 0.001(0.001)	− 0.002(0.001)
VPD > 2 kPa	− 1.4(0.8)	− 1.2(3.2)	− 1.7(1.5)	− 1.6(1.2)	1.4(0.9)	1.2(3.0)	3.0(1.3)	0.3(0.6)	− 0.060(0.070)	− 0.060(0.030)	− 0.001(0.001)	− 0.001(0.002)

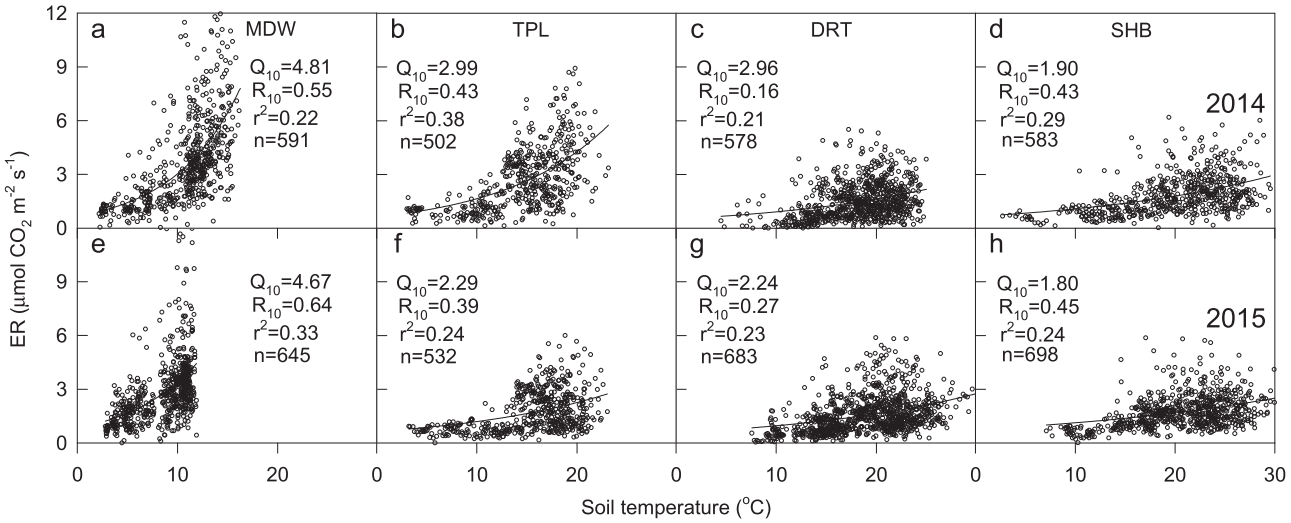

Fig. 5. Response of nighttime ecosystem respiration (ER) to soil temperature at 100 mm depth at MDW (a, e), TPL (b, f), DRT (c, g) and SHB (d, h) during the two growing seasons in 2014 and 2015. R_{10} is the respiration (μmol CO_2 m^{-2} s^{-1}) at the reference soil temperature of 10 °C and Q_{10} is the respiration temperature sensitivity coefficient.

DRT and SHB, respectively; α was reduced as well.

3.3.2. Responses of nighttime NEE to soil temperature

The exponential relationships between nighttime NEE (ER) and T_s were detected based on nighttime data during the growing season in both years (Fig. 5). Comparison of the four ecosystems showed that ER at MDW was more sensitive to T_s change than at the other three ecosystems. The temperature sensitivity of ER (Q_{10}) was estimated to be 1.8–4.8 during the growing period, with the highest Q_{10} at MDW and the lowest at SHB. The ER at reference temperature (R_{10}) was highest at MDW (0.60 μmol CO_2 m^{-2} s^{-1}) and the lowest at DRT (0.24 μmol CO_2 m^{-2} s^{-1}). The R_{10} in TPL and SHB was very close to the mean value of 0.43 μmol CO_2 m^{-2} s^{-1}.

3.4. Daily, seasonal and annual variations in GEP, ER and NEE

NEE, ER, and GEP for different ecosystems showed similar seasonal changes, which were closely related to the growth and phenology of vegetation in the two years (Fig. 6 vs Fig. 2). NEE, ER, and GEP values and the variations were much lower at DRT and SHB than at MDW and TPL. The minimum daily NEE values were −4.9, −1.9, −1.7 and −1.4 g C m^{-2} d^{-1} at MDW, TPL, DRT and SHB, respectively, in July or August. The maximum ER was 7.5, 5.8, 3.4 and 3.0 g C m^{-2} d^{-1}, while the maximum GEP was 9.2, 6.3, 5.8 and 3.9 g C m^{-2} d^{-1}.

All four sites were *C* sources at the annual scale, with 69, 157, 166 and 177 g C m^{-2} at MDW, TPL, DRT and SHB, respectively (Table 2). The annual GPP/ER ratio in these four ecosystems was always <1, which also demonstrates their *C*-source nature. During the growing season, the NEE was −84, −2, 9 and 43 g C m^{-2}, respectively, as MDW acted as a *C* sink, TPL and DRT as *C* neutral, and SHB as a *C* source. The integrated order of GEP and ER in each ecosystem was greater at MDW, followed by TPL and DRT, and SHB. MDW had the highest GEP and ER, resulting in the highest *C* assimilation during the growing season and lowest *C* release in both years among the four ecosystems (Fig. 7, Table 2). SHB had the lowest GEP, but the highest *C* release. The annual GEP and ER varied widely among sites and years. Annual ER ranged

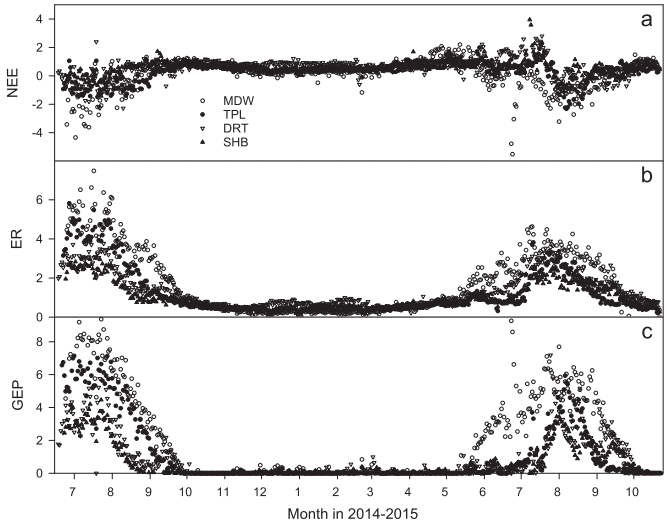

Fig. 6. Seasonal change in daily carbon fluxes (g C m^{-2} yr^{-1}) of the net ecosystem exchange (NEE), ecosystem respiration (ER), and gross ecosystem production (GEP) in the four ecosystems.

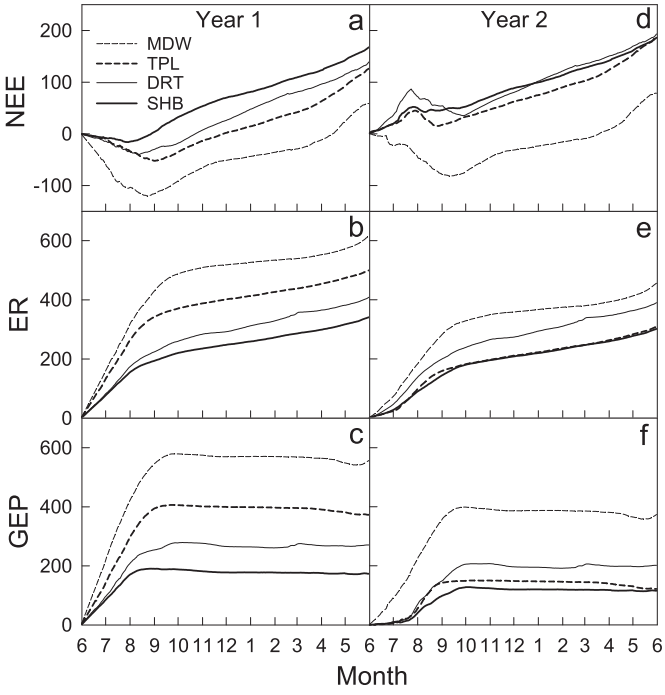

Fig. 7. Two year accumulative variations in carbon fluxes (g C m^{-2} d^{-1}) of the net ecosystem CO_2 exchange (NEE), ecosystem respiration (ER), and gross ecosystem production (GEP) in the four ecosystems on the Mongolian Plateau in 2014 and 2015.

from 302 g m^{-2} (SHB in 2015) to 616 g m^{-2} (MDW in 2014), and GEP ranged from 116 to 557 g m^{-2} at the same sites.

4. Discussion

4.1. Abiotic regulation of daytime NEE

MDW – the typical grasslands under permafrost – had the strongest *C* assimilation potential when compared to the other three ecosystems under the same T_a, SWC, and VPD conditions (Fig. 4). Temperature influences photosynthesis and respiration of plants primarily via temperature-dependent Rubisco enzyme activity (Farquhar et al., 1980; Turner et al., 1985). In our study, the optimum T_a for NEE_{max} appeared to be 10–20 °C (Table 3), which is ~5 °C lower than that reported by Zhang et al. (2007) at a temperature steppe on the southern Mongolian Plateau. A significant reduction in *C* assimilation was found when T_a was > 20 °C in all four ecosystems, but at a much lower reduction compared to when T_a was < 10 °C, showing low temperature adaptation of vegetative communities in the northern rather than southern Plateau. When T_a increased, the NEE of both MDW and TPL changed at a greater rate than at DRT and SHB, indicating not only a stronger *C* release potential but also a higher temperature sensitivity at MDW and TPL. The ongoing and predicted global warming trend in Mongolia (Lu et al., 2009; Chen et al., 2013) would more likely affect the MDW and TPL instead of the DRT and SHB.

SHB showed a higher NEE_{max} and α under drought conditions (SWC < 15%, Table 3), suggesting that plant species in the shrublands have higher tolerance to drought stress, though greater *C* assimilation potential and light use efficiency were observed at MDW and TPL under wet soil moisture conditions (SWC > 15%). Shrubland plants with high drought tolerance present substantial advantages over drought intolerant plants, compensating the effects of reduced water availability (Valladares and Pearcy, 1997; Han et al., 2014). The tolerance of plant species to drought is a common phenomenon in dryland regions (Lei et al., 2015, 2016). The result of *C* assimilation potential decrease with decreasing SWC in the four sites (Table 3) was consistent with the results from our earlier study of a desert steppe (Shao et al., 2013).

Both the NEE and NEE_{max} of our ecosystems decreased with increases in VPD because the increase in VPD decreased the leaf conductance and assimilation rate (Turner et al., 1985; Chen et al., 2002). At a higher VPD, NEE is decreased because of stomatal closure under drought conditions (Farquhar et al., 1980; Chen et al., 2002). The changes of NEE_{max} in the steppe with VPD at DRT and SHB were much smaller than that at MDW and TPL, suggesting a stronger VPD dependence for the latter two ecosystems and further emphasizing not only a stronger *C* assimilation potential but also a higher relative environmental sensitivity of MDW and TPL.

4.2. Biophysical regulations on seasonality of GEP, ER and NEE

The seasonal variations in GEP, ER and NEE at MDW were dominated by T_a (Table 4). Temperature had the most significant influence at MDW on both ecosystem activity (Mano et al., 2003; Ouyang et al., 2014) and on *C* flux dynamics out of the other three ecosystems because MDW experienced low temperatures and a high SWC (Table 3, Fig. 5a and e), as reported in alpine meadows (Kato and Tang, 2008; Fu et al., 2009) and tundra (Huemmrich et al., 2010). At MDW, both T_a and T_s were ~4 °C lower than at the other three sites (Table 2); even in late June of 2015, melting ice was found at an ~1 m depth permafrost table, where sufficient permafrost melting water refilled the soil. The higher SWC, related to the more physiologically active leaves at MDW compared to other three water-limited sites (Fig. 2), produced a greater GEP and ER, and a longer duration of *C* assimilation (Fig. 6). However, this refilling process may come to a stop with the disappearance of permafrost. Our results suggest that *C* fluxes in meadows are largely influenced by temperature (Kato et al., 2006; Fu et al., 2009).

SWC was the primary factor affecting seasonal variation in *C* fluxes at TPL, DRT, and SHB (Table 4). The ecosystem activity at these three drier sites were potentially affected by a low annual SWC – 6.5% at DRT and SHB, 7.3% at TPL – as seen in comparison to MDW's annual SWC of 37.6% (Table 2). Generally, water deficits cause a decline in net *C* assimilation and lead to a decrease in internal leaf CO_2 concentrations through adjusted closed leaf stomata (Farquhar et al., 1980; Buckley and Mott, 2002). As a result, the seasonal variation of GEP, ER and NEE at these three sites were directly and significantly correlated with SWC (Table 4). Our conclusions based on monthly data were consistent with previous studies that SWC was the primary factor controlling seasonal and inter-annual variations in *C* fluxes across the Mongolian steppes (Wang et al., 2008; Shao et al., 2013) and in other water-limited grasslands (Flanagan et al., 2002; Ma et al., 2007; Li et al., 2012).

4.3. Mongolian carbon sequestration in a global context with nomadic implications

A large variability exists in global grassland *C* sequestration based on the FLUXNET synthesis, primarily due to diverse vegetation, climate, soil and disturbance types (including land use) (Kato and Tang, 2008; Li et al., 2013; Xiao et al., 2013; Ahlström et al., 2015). In our study, the four sites represented four major vegetation succession types on the Mongolian Plateau. MDW acted as a *C* sink, TPL and DRT as *C* neutral, while SHB as a *C* source within the two growing seasons (Fig. 8a). The minimum daily (−5.5 to −1.4 g C m^{-2} d^{-1}) and seasonal sum NEEs (−92–53 g C m^{-2}) at these four sites were within the range of values reported for grasslands (Soegaard et al., 2003; Li et al., 2005; Ahlström et al., 2015). Annual NEEs varying from 59 to 193 g C m^{-2} with a mean of 142 ± 48 g C m^{-2} within the annual NEE ranges were reported for grasslands elsewhere (−366–481 g C m^{-2}) (Gilmanov et al., 2007, 2010), albeit all four sites acted as a *C* source.

In general, a longer growing season would cause a greater *C* assimilation. Following the method of Chu et al. (2015), i.e., assuming three continuous *C* sink/source days as the beginning/ending of a growing season, the growing season length (GSL) was 92, 60, 59 and 34 days at MDW, TPL, DRT and SHB, respectively. This indicates that the GSL at SHB was about one third of MDW, and half of TPL or DRT, suggesting that the differences in the overall phenological period were tightly related to *C* fluxes. These results supported our previous finding that a longer growing season is responsible for the greater *C* assimilation (Shao et al., 2013). The annual *C* assimilation in the four grassland ecosystems was less than that of the North American tall-grass prairies, which had higher precipitation (Zenone et al., 2011), and that of the intensively managed grasslands in central and northern Europe (Soussana et al., 2007).

Substantial land cover and land use changes have occurred in the Mongolian grasslands over the last half-century, resulting in significant ecological and socioeconomic consequences (Han et al., 2009; Chen et al., 2013; John et al., 2016), such as *C* sequestration shifts. In our sites, a conversion from MDW to SHB would increase *C* release by 2.6-fold; MDW to TPL would increase *C* release by 2.2-fold, and TPL to SHB would increase *C* release by 1.1-fold at an annual time scale. These results provide evidence of the significant *C* exchange shifts among different grassland ecosystems.

We selected a few EC-based studies on the Mongolian Plateau and nearby regions for comparison (Table 5). Studies on *C* fluxes in meadows of the Mongolian Plateau were rare. We found that the *L.chinensis* meadow steppe was an annual source of 59 g C m^{-2}, while Dong et al. (2011) found a *C* sink which had a much higher LAI. Our results were comparable with those of another meadow steppe in the south of the Qinghai-Tibet Plateau, which had similar LAI and an NEE of 55 g C m^{-2} (Fu et al., 2009), suggesting that meadow steppe *C* fluxes might be controlled by LAI. The growing seasonal NEE of −36–36 g C m^{-2} at TPL and DRT (Table 2) was similar to that of a temperate steppe with a similar LAI, varying from −12 to 20 g C m^{-2} in 2004–2006 (Wang

Table 4
Statistical information regression coefficient (Coef.) and constant (Cons.), partial correlation coefficient (partial *r*) and significance probability (*P*) for the relationships between ecosystem *C* fluxes (NEE, ER, and GEP) and air temperature (T_a), soil moisture (SWC), photosynthetically active radiation (PAR), rainfall and green above ground biomass (GNPP) using a stepwise multiple linear regression analysis at the four grassland ecosystems. The monthly data during growing seasons in 2014 and 2015 were used. $P < 0.05$, 0.01, and 0.001 indicated by *, **, and ***, respectively.

Site	Factors	Coef.	NEE Partial *r*	*P*	Coef.	ER Partial *r*	*P*	Coef.	GEP Partial *r*	*P*
MDW	Cons.	46.72		0.002**	32.27		0.01*	−32.41		0.06
	T_a	−3.13	−0.76	0.03*	0.29	0.68	0.05*	6.07	0.83	0.01**
	SWC	−0.33	−0.53	0.22	−0.05	−0.16	0.70	0.11	0.54	0.21
	PAR	0.24	0.57	0.24	0.11	0.33	0.42	−0.14	−0.52	0.23
	Rainfall	0.27	0.40	0.43	0.50	0.77	0.02*	0.14	0.35	0.44
	GNPP	−80.91	−0.80	0.02*	224.02	0.95	<0.001***	254.26	0.95	<0.001***
TPL	Cons.	25.8		0.01**	−22.22		0.02*	−101.22		0.001***
	T_a	−0.29	−0.38	0.28	0.04	0.27	0.51	0.15	0.35	0.33
	SWC	−3.30	−0.68	0.04*	0.46	0.87	0.002**	14.26	0.94	<0.001***
	PAR	−0.11	−0.27	0.68	0.02	0.16	0.70	0.01	0.01	0.86
	Rainfall	−0.25	−0.42	0.45	0.46	0.88	0.002**	0.22	0.25	0.49
	GNPP	−47.72	−0.71	0.01**	0.14	0.76	0.02*	0.26	0.59	0.05*
DRT	Cons.	49.17		0.01**	−28.56		0.003**	−102.48		<0.001***
	T_a	−0.11	−0.12	0.75	−0.04	−0.25	0.55	0.04	0.14	0.73
	SWC	−4.58	−0.72	0.01*	6.70	0.92	<0.001***	14.31	0.95	<0.001***
	PAR	0.13	0.16	0.65	−0.02	−0.17	0.68	−0.06	−0.26	0.50
	Rainfall	0.49	0.27	0.45	0.76	0.88	0.002**	0.06	0.10	0.28
	GNPP	−0.42	−0.49	0.16	17.49	0.75	0.01*	51.92	0.71	0.02*
SHB	Cons.	47.16		0.04*	−42.36		0.08	−84.39		0.06
	T_a	−0.07	−0.11	0.85	0.50	0.63	0.05*	0.46	0.54	0.11
	SWC	−4.07	−0.82	0.04*	8.70	0.82	0.002**	11.30	0.70	0.01*
	PAR	0.15	0.24	0.69	0.30	0.44	0.21	0.27	0.32	0.37
	Rainfall	−0.36	−0.52	0.37	0.48	0.61	0.05*	0.40	0.41	0.24
	GNPP	−0.01	−0.02	0.98	0.37	0.63	0.05*	0.36	0.50	0.14

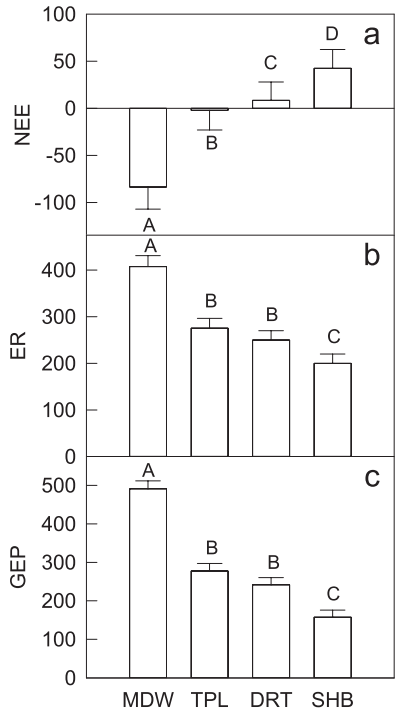

Fig. 8. Sum of the two growing seasonal (June–September) carbon fluxes (g C m^{-2} season^{-1}) of the net ecosystem CO_2 exchange (NEE, a), ecosystem respiration (ER, b), and gross ecosystem production (GEP, c). Significant differences between ecosystems are indicated by different letters at $P = 0.05$.

et al., 2008). Furthermore, annual GEP, ER and NEE were comparable to another grassland south of the Mongolian Plateau that also had a similar LAI and NEE of 124 g C m^{-2} in 2004–2005 (Fu et al., 2009). The only available publication within the same region (Li et al., 2005) was conducted at a typical steppe in 2003, where the authors reported a *C* neutral or a minor sink. However, the annual precipitation was much higher (244 mm) than for either year at our study sites. Our study, for the first time, included the *A. splendens* dry steppe – a widely-distributed cover type characterized by overgrazing in Mongolia, which appeared as an annual *C* source (166 g C m^{-2}). Supposing this DRT changed from a MDW due to global warming and/or overgrazing, this would mean a 2.4 fold increase of *C* release. Zhao et al. (2006) and Fu et al. (2009) found that alpine shrublands acted as a *C* sink (−52 and −596 g C m^{-2} yr^{-1}, respectively), whereas we observed a *C* source both during the individual growing season and at the annual scale. Compared to our sites, the annual mean precipitation of their sites were > 500 mm and the SWC was significantly higher, indicating that SWC was the main reason for the *C* budget differences in the shrublands (Table 5).

In sum, the Mongolian Plateau possesses a variety of *C* flux regimes owing to its different vegetation type, soil, and climate (Liu et al., 2014). It is a very sensitive biogeographical area due to its semi-arid environment and vast coverage area (Li et al., 2005). Our results show that management (e.g., fires) may be necessary to enhance the resilience of shrubs, and to impose a shift from shrubland to grassland (Rostagno et al., 2006; Gower et al., 2015). Grassland management may also be needed (Lafortezza and Chen, 2016; Smiraglia et al., 2016), which leads to an increase in *C* assimilation ability and ecosystem productivity (Wangchuk et al., 2013; Ahlström et al., 2015) as well as the mediation of the global warming (Woodward and Kelly, 2008; Gilmanov et al., 2010).

A large proportion of the rural population in Mongolia is made up of nomadic herders, who are vulnerable to the effects of vegetation changes on forage cover and productivity (Angerer et al., 2008). The collapse of the former Soviet Union resulted in the privatization of the state owned herds (Chen et al., 2015a) and a sharp increase in livestock stocking rates (John et al., 2016). Several studies have linked the level of degradation in the Mongolian grasslands to the increase in livestock and the proportion of goats to sheep, which might increase the degree

Table 5
Comparison of ecosystem characteristics and *C* fluxes of eddy covariance (EC) measurements on the Mongolian Plateau or the nearby dryland Eurasian steppe area. LAI, leaf area index; NEE, net ecosystem CO_2 exchange. Unit is μmol CO_2 m^{-2} s^{-1} for min and max NEE, g C m^{-2} d^{-1} for daily NEE, and g C m^{-2} yr^{-1} for annual NEE. NA, data not available.

Ecosystem type	Year	LAI	Min NEE	Max NEE	Min daily NEE	Annual NEE	Source
Leymus chinensis meadow steppe	2007–2008	2.9–3.1	−16.7	4.0	−6.3	−160 to −64	(Dong et al., 2011)
Leymus chinensis meadow steppe	2009–2013	NA	NA	NA	−4.0	−150 to −62	(Qu et al., 2016)
Potentilla fruticisa L.shrub-meadow	2004–2005	2.6–2.7	NA	NA	NA	−52 to −85	(Fu et al., 2009)
Stipa capillacea meadow steppe	2004–2005	0.7–1.0	NA	NA	NA	37–55	
Leymus chinensis temperature steppe	2004–2005	0.5–1.0	NA	NA	NA	107–140	
Stipa krylovii temperature steppe	2003	0.6	−3.6	1.2	−2.3	−41	(Li et al., 2005)
Stipa krylovii temperature steppe	2004–2006	0.8–1	−8 to −3	NA	NA	37–68	(Wang et al., 2008)
Stipa klemenzii desert steppe	2008–2010	0.4–0.5	NA	NA	−1.6	−23–26	(Yang et al., 2011)
Stipa breviflora desert steppe	2010	0.7	−2.4	1.5	−0.9	43	(Shao et al., 2013)
Stipa breviflora desert steppe	2011	0.4	−3.8	1.0	−1.5	48	
Leymus chinensis meadow steppe	2014	0.9	−7.9	5.4	−4.3	59	This study
	2015		−6.9	3.7	−5.5	79	
Stipa krylovii temperature steppe	2014	1.0	−6.2	4.8	−1.5	126	
	2015		−4.7	2.2	−2.3	187	
Achnatherum splendens dry steppe	2014	1.0	−4.3	3.8	−1.7	139	
	2015		−5.0	3.1	−1.8	193	
Caragana stenophylla shrubland	2014	0.8	−3.4	3.4	−1.4	168	
	2015		−3.0	2.4	−1.4	186	

of degradation (Hilker et al., 2014). Fernandez-Gimenez (2000) suggested that the meadow steppe (*C*-sink) responds to the equilibrium or range control theory of grassland dynamics, where the grazing pressure heavily influences vegetation dynamics in addition to abiotic controls, while the dry steppe and typical steppe both respond to highly variable precipitation and soil moisture. This suggests that disturbances (e.g., grazing and other land use) might cause above ground biomass reduction and soil erosion, consequentially resulting in a significant vegetation change. The reduced cover and eroded soil might facilitate a transition to a more resilient, typical steppe, and finally to a dry steppe species (*C*-source) such as shrubs dominating the landscape, which would have a deleterious effect on the regional *C* balance. The maintenance of the human-nature balance in the context of ongoing global changes is increasingly challenging these days. From the standpoint of *C* sequestration and grassland productivity, a baseline assessment of ecological status and continued monitoring of Mongolian grasslands changes can provide ecologically-sound grassland management strategies.

5. Conclusions

For the first time, we developed a cluster of four eddy covariance towers in Mongolia to quantify how *C* fluxes shift among four different dominant ecosystems and their physical regulations at the high-latitude ecological area of the northern Mongolian Plateau. All four sites acted as a *C* source at the annual scale; however, during the two growing seasons, meadow steppe acted as a *C* sink, temperate and dry steppes as *C* neutral, and shrubland as a *C* source. At an annual time scale, meadow-to-shrub and typical steppe conversions would result in a 2.6- and 2.2-fold increase in *C* release, respectively, whereas a typical steppe-to-shrub conversion would result in a 1.1-fold increase. Meadow steppe was more greatly affected by temperature, while both the typical steppe and shrubland were more greatly affected by water status. With increasing land use and drought intensity, a clear trend of increased CO_2 emissions will result in further global warming, which should be taken into consideration by natural resource management departments and policy makers.

Acknowledgements

This study was supported by the LCLUC program of NASA (NNX15AD10G), the “Dynamics of Coupled Natural and Human Systems (CNH)” Program of the NSF (#1313761), and the USCCC. We appreciate the careful editing of Gabriela Shirkey.

References

Abraha, M., et al., 2016. Ecosystem water use efficiency of annual corn and perennial grasslands: contributions from land use history and species composition. Ecosystems 19, 1001–1012.
Ahlström, A., et al., 2015. The dominant role of semi-arid ecosystems in the trend and variability of the land CO_2 sink. Science 348, 895–899.
Angerer, J., et al., 2008. Climate change and ecosystems of Asia with emphasis on Inner Mongolia and Mongolia. Rangelands 30, 46–51.
Aurela, M., et al., 2002. Annual CO_2 balance of a subarctic fen in northern Europe: importance of the wintertime efflux. J. Geophys. Res. -Atmos. 107, 1–12.
Buckley, T.N., Mott, K.A., 2002. Dynamics of stomatal water relations during the humidity response: implications of two hypothetical mechanisms. Plant Cell Environ. 25, 407–419.
Burba, G.G., et al., 2008. Addressing the influence of instrument surface heat exchange on the measurements of CO_2 flux from open-path gas analyzers. Glob. Change Biol. 14, 1854–1876.
Chen, J.Q., et al., 2002. Biophysical controls of carbon flows in three successional Douglas-fir stands based on eddy-covariance measurements. Tree Physiol. 22, 169–177.
Chen, J.Q., et al., 2013. Dryland East Asia (DEA): Land Dynamics Amid Social and Climate Change. HEP and De Gruyter, Beijing.
Chen, J.Q., et al., 2015a. Policy shifts influence the functional changes of the CNH systems on the Mongolian Plateau. Environ. Res. Lett. 10. http://dx.doi.org/10.1088/1748-9326/10/8/085003.
Chen, J.Q., et al., 2015b. Divergences of two coupled human and natural systems on the Mongolian Plateau. Bioscience 65, 559–570.
Chu, H., et al., 2014. Net ecosystem CH_4 and CO_2 exchanges in a Lake Erie coastal marsh and a nearby cropland. J. Geophys. Res.-Biogeosci. 119, 722–740.
Chu, H., et al., 2015. Climatic variability, hydrologic anomaly, and methane emission can turn productive freshwater marshes into net carbon sources. Glob. Change Biol. 21, 1165–1181.
Dangal, S.R.S., et al., 2016. Synergistic effects of climate change and grazing on net primary production of Mongolian grasslands. Ecosphere 7, 1–20.
Dong, G., et al., 2011. Effects of spring drought on carbon sequestration, evapotranspiration and water use efficiency in the songnen meadow steppe in northeast China. Ecohydrology 4, 211–224.
Eggermont, H., et al., 2015. Nature-based solutions: new influence for environmental management and research in Europe. Gaia-Ecol. Perspect. Sci. Soc. 24, 243–248.
European Commission, 2010. Communication from the commission to the European parliament, the council, the European economic and social committee and the committee of the regions. Europe 2020 Flagship Initiative Innovation Union.
Falge, E., et al., 2001. Gap filling strategies for defensible annual sums of net ecosystem exchange. Agric. For. Meteorol. 107, 43–69.
Farquhar, G.D., et al., 1980. Responses to humidity by stomata of *Nicotiana-glauca L* and *Corylus-avellana L* are consistent with the optimization of carbon-dioxide uptake with respect to water-loss. Aust. J. Plant Physiol. 7, 315–327.
Fernandez-Gimenez, M.E., 2000. The role of Mongolian nomadic pastoralists' ecological knowledge in rangeland management. Ecol. Appl. 10, 1318–1326.
Fernández-Giménez, M.E., et al., 2012. Cross-boundary and cross-level dynamics increase vulnerability to severe winter disasters (dzud) in Mongolia. Glob. Environ. Change 22, 836–851.
Flanagan, L.B., et al., 2002. Seasonal and interannual variation in carbon dioxide exchange and carbon balance in a northern temperate grassland. Glob. Change Biol. 8, 599–615.
Foken, T., 2008. The energy balance closure problem: an overview. Ecol. Appl. 18, 1351–1367.

Fu, Y.L., et al., 2009. Environmental influences on carbon dioxide fluxes over three grassland ecosystems in China. Biogeosciences 6, 2879–2893.
Gilmanov, T.G., et al., 2007. Partitioning European grassland net ecosystem CO_2 exchange into gross primary productivity and ecosystem respiration using light response function analysis. Agric. Ecosyst. Environ. 121, 93–120.
Gilmanov, T.G., et al., 2010. Productivity, respiration, and light-response parameters of world grassland and agroecosystems derived from flux-tower measurements. Rangel. Ecol. Manag. 63, 16–39.
Gower, K., et al., 2015. Sequential disturbance effects of hailstorm and fire on vegetation in a mediterranean-type ecosystem. Ecosystems 18, 1121–1134.
Groisman, P., Soja, A.J., 2009. Ongoing climatic change in Northern Eurasia: justification for expedient research. Environ. Res. Lett. 4. http://dx.doi.org/10.1088/1748-9326/4/4/045002.
Han, J., et al., 2014. Legacy effects from historical grazing enhanced carbon sequestration in a desert steppe. J. Arid Environ. 107, 1–9.
Han, X.G., et al., 2009. The grasslands of Inner Mongolia: a special feature. Rangel. Ecol. Manag. 62, 303–304.
Hilker, T., et al., 2014. Satellite observed widespread decline in Mongolian grasslands largely due to overgrazing. Glob. Change Biol. 20, 418–428.
Huemmrich, K.F., et al., 2010. Tundra carbon balance under varying temperature and moisture regimes. J. Geophys. Res.-Biogeosci. 115. http://dx.doi.org/10.1029/2009jg001237.
IPCC, 2014. Climate Change 2014: Synthesis Report. In: Core Writing Team, Pachauri, R.K., Meyer, L.A. (Eds.), Contribution of Working Groups I, II and III to the Fifth Assessment Report of the Intergovernmental Panel on Climate Change. IPCC, Geneva, Switzerland, pp. 151.
John, R., et al., 2009. Land cover/land use change in semi-arid Inner Mongolia: 1992–2004. Environ. Res. Lett. 4. http://dx.doi.org/10.1088/1748-9326/4/4/045010.
John, R., et al., 2016. Differentiating anthropogenic modification and precipitation-driven change on vegetation productivity on the Mongolian Plateau. Landsc. Ecol. 31, 547–566.
Kato, T., et al., 2006. Temperature and biomass influences on interannual changes in CO_2 exchange in an alpine meadow on the Qinghai-Tibetan Plateau. Glob. Change Biol. 12, 1285–1298.
Kato, T., Tang, Y.H., 2008. Spatial variability and major controlling factors of CO_2 sink strength in Asian terrestrial ecosystems: evidence from eddy covariance data. Glob. Change Biol. 14, 2333–2348.
Kelley, C.P., et al., 2015. Climate change in the Fertile Crescent and implications of the recent Syrian drought. Proc. Natl. Acad. Sci. USA 112, 3241–3246.
Kormann, R., Meixner, F., 2001. An analytical footprint model for non-neutral stratification. Bound. -Lay. Meteorol. 99, 207–224.
Lafortezza, R., Chen, J.Q., 2016. The provision of ecosystem services in response to global change: evidences and applications. Environ. Res. 147, 576–579.
Lei, T., et al., 2015. A new framework for evaluating the impacts of drought on net primary productivity of grassland. Sci. Total Environ. 536, 161–172.
Lei, T., et al., 2016. Drought and carbon cycling of grassland ecosystems under global change: a review. Water 8. http://dx.doi.org/10.3390/w8100460.
Li, S.G., et al., 2005. Net ecosystem carbon dioxide exchange over grazed steppe in central Mongolia. Glob. Change Biol. 11, 1941–1955.
Li, X., et al., 2012. Estimation of evapotranspiration over the terrestrial ecosystems in China. Ecohydrology 7, 139–149.
Li, X., et al., 2013. Estimation of gross primary production over the terrestrial ecosystems in China. Ecol. Model. 261–262, 80–92.
Lioubimtseva, E., Henebry, G.M., 2009. Climate and environmental change in arid Central Asia: impacts, vulnerability, and adaptations. J. Arid Environ. 73, 963–977.
Liu, Y., et al., 2014. Response of evapotranspiration and water availability to the changing climate in Northern Eurasia. Clim. Change 126, 413–427.
Lloyd, J., Taylor, J.A., 1994. On the temperature-dependence of soil respiration. Funct. Ecol. 8, 315–323.
Lu, N., et al., 2009. Climate change in Inner Mongolia from 1955 to 2005 – trends at regional, biome and local scales. Environ. Res. Lett. 4. http://dx.doi.org/10.1088/1748-9326/4/4/045006.
Luo, C., Wu, D., 2016. Environment and economic risk: an analysis of carbon emission market and portfolio management. Environ. Res. 149, 297–301.
Ma, S.Y., et al., 2007. Inter-annual variability in carbon dioxide exchange of an oak/grass savanna and open grassland in California. Agric. For. Meteorol. 147, 157–171.
Maes, J., Jacobs, S., 2015. Nature-based solutions for. Eur. Sustain. Dev. Conserv. Lett. 1–4.
Mano, M., et al., 2003. Net CO_2 budget and seasonal variation of CO_2 fluxes at a wet sedge tundra ecosystem at Barrow, Alaska during the 2000 growing season. J. Agric. Meteorol. 59, 141–154.
Moncrieff, J., et al., 2004. Averaging, detrending, and filtering of eddy covariance time series. In: Lee, X., Massman, W., Law, B. (Eds.), Handbook of Micrometeorology: A Guide for Surface Flux Measurement and Analysis. Kluwer Acadamic, Dordrecht, Netherlands, pp. 7–32.
Ouyang, Z., et al., 2014. Disentangling the confounding effects of PAR and air temperature on net ecosystem exchange at multiple time scales. Ecol. Complex. 19, 46–58.
Qi, J., et al., 2012. Understanding the coupled natural and human systems in Dryland East Asia. Environ. Res. Lett. 7. http://dx.doi.org/10.1088/1748-9326/7/1/015202.
Qi, J., et al., 2017. Understanding livestock production and sustainability of grassland ecosystems in the Asian Dryland Belt. Ecol. Process. 6. http://dx.doi.org/10.1186/s13717-017-0087-3.
Qu, L., et al., 2016. Heat waves reduce ecosystem carbon sink strength in a Eurasian meadow steppe. Environ. Res. 144, 39–48.
Reichstein, M., et al., 2005. On the separation of net ecosystem exchange into assimilation and ecosystem respiration: review and improved algorithm. Glob. Change Biol. 11, 1424–1439.
Rostagno, C.M., et al., 2006. Postfire vegetation dynamics in three rangelands of northeastern Patagonia, Argentina. Rangel. Ecol. Manag. 59, 163–170.
Shao, C., et al., 2008. Spatial variability in soil heat flux at three Inner Mongolia steppe ecosystems. Agric. For. Meteorol. 148, 1433–1443.
Shao, C., et al., 2012. Ecosystem responses to mowing manipulations in an arid Inner Mongolia steppe: an energy perspective. J. Arid Environ. 82, 1–10.
Shao, C., et al., 2013. Grazing alters the biophysical regulation of carbon fluxes in a desert steppe. Environ. Res. Lett. 8. http://dx.doi.org/10.1088/1748-9326/8/2/025012.
Shao, C., et al., 2014. Spatial variation of net radiation and its contribution to energy balance closures in grassland ecosystems. Ecol. Process. 3, 1–11.
Shao, C., et al., 2017. Grazing effects on surface energy fluxes in a desert steppe on the Mongolian Plateau. Ecol. Appl. 27, 485–502.
Smiraglia, D., et al., 2016. Linking trajectories of land change, land degradation processes and ecosystem services. Environ. Res. 147, 590–600.
Soegaard, H., et al., 2003. Carbon dioxide exchange over agricultural landscape using eddy correlation and footprint modelling. Agric. For. Meteorol. 114, 153–173.
Soussana, J.F., et al., 2007. Full accounting of the greenhouse gas (CO_2, N_2O, CH_4) budget of nine European grassland sites. Agicr. Ecosyst. Environ. 121, 121–134.
Turner, N.C., et al., 1985. The responses of stomata and leaf gas-exchange to vapor-pressure deficits and soil-water content. 2. in the mesophytic herbaceous species helianthus-annuus. Oecologia 65, 348–355.
Valladares, F., Pearcy, R.W., 1997. Interactions between water stress, sun-shade acclimation, heat tolerance and photoinhibition in the sclerophyll Heteromeles arbutifolia. Plant Cell Environ. 20, 25–36.
Wang, Y.L., et al., 2008. Environmental effects on net ecosystem CO_2 exchange at half-hour and month scales over Stipa krylovii steppe in northern China. Agric. For. Meteorol. 148, 714–722.
Wangchuk, K., et al., 2013. Shrubland or Pasture? Restoration of Degraded Meadows in the Mountains of Bhutan. Mt. Res. Dev. 33, 161–169.
Webb, E.K., et al., 1980. Correction of flux measurements for density effects due to heat and water-vapor transfer. Q. J. R. Meteor. Soc. 106, 85–100.
Wilczak, J.M., et al., 2001. Sonic anemometer tilt correction algorithms. Bound. -Lay. Meteorol. 99, 127–150.
Wilson, K.B., et al., 2002. Energy partitioning between latent and sensible heat flux during the warm season at FLUXNET sites. Water Resour. Res. 38, 1294–1304.
Woodward, F.I., Kelly, C.K., 2008. Responses of global plant diversity capacity to changes in carbon dioxide concentration and climate. Ecol. Lett. 11, 1229–1237.
Xiao, J., et al., 2013. Carbon fluxes, evapotranspiration, and water use efficiency of terrestrial ecosystems in China. Agric. For. Meteorol. 182–183, 76–90.
Xie, J., et al., 2014. Long-term variability and environmental control of the carbon cycle in an oak-dominated temperate forest. For. Ecol. Manag. 313, 319–328.
Yang, F.L., et al., 2011. Biophysical regulation of net ecosystem carbon dioxide exchange over a temperate desert steppe in Inner Mongolia. China Agric. Ecosyst. Environ. 142, 318–328.
Yuan, W.P., et al., 2007. Deriving a light use efficiency model from eddy covariance flux data for predicting daily gross primary production across biomes. Agric. For. Meteorol. 143, 189–207.
Zenone, T., et al., 2011. CO_2 fluxes of transitional bioenergy crops: effect of land conversion during the first year of cultivation. GCB Bioenergy 3, 401–412.
Zhang, F., et al., 2014. Estimating canopy characteristics of Inner Mongolia's grasslands from field spectrometry. Remote Sens. 6, 2239–2254.
Zhang, W.L., et al., 2007. Biophysical regulations of carbon fluxes of a steppe and a cultivated cropland in semiarid Inner Mongolia. Agric. For. Meteorol. 146, 216–229.
Zhao, L., et al., 2006. Diurnal, seasonal and annual variation in net ecosystem CO_2 exchange of an alpine shrubland on Qinghai-Tibetan plateau. Glob. Change Biol. 12, 1940–1953.